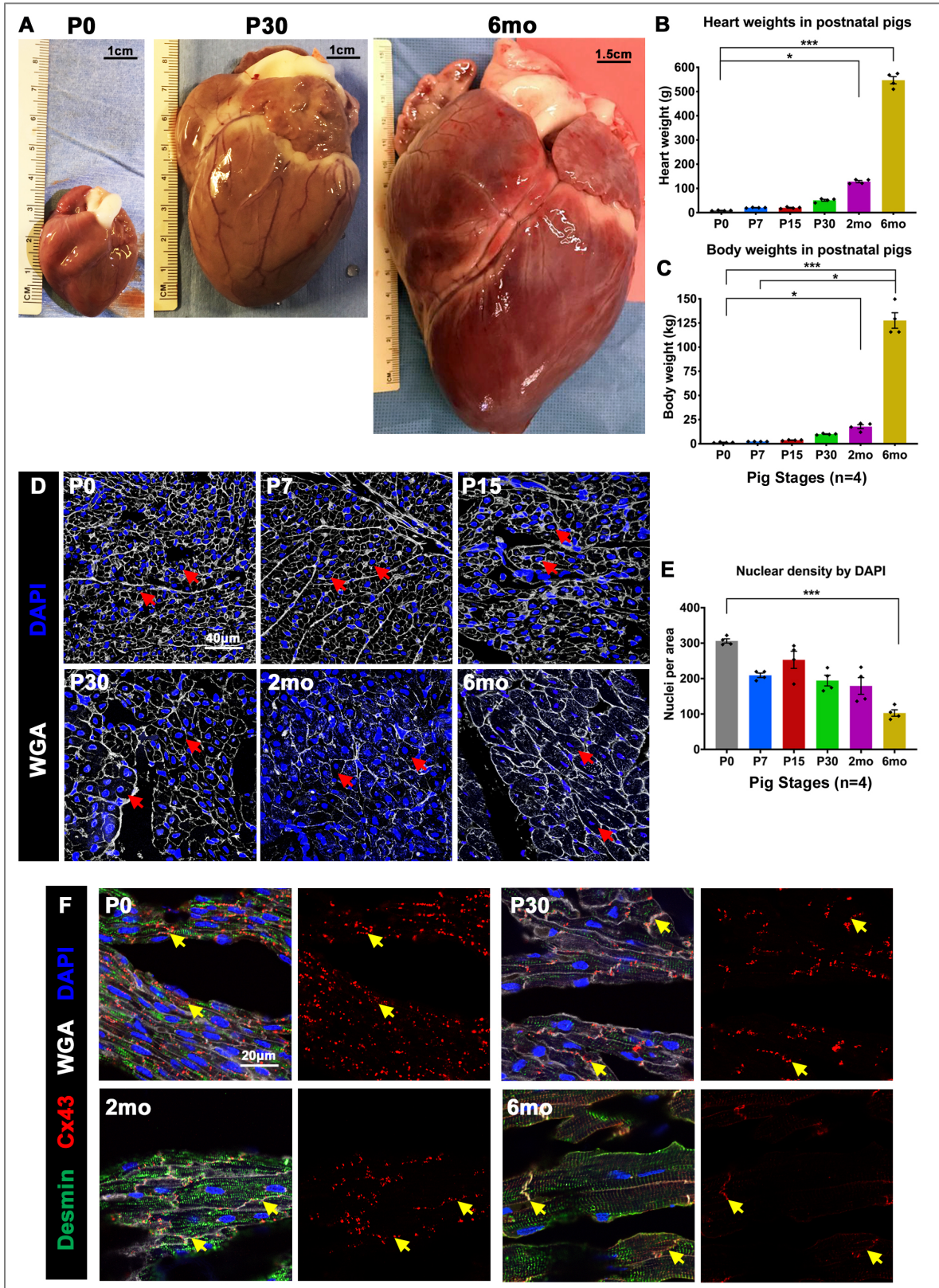


SUPPLEMENTARY INFORMATION

**Velayutham *et al.*,
'Cardiomyocyte cell cycling, maturation, and growth by multinucleation in
postnatal swine'**

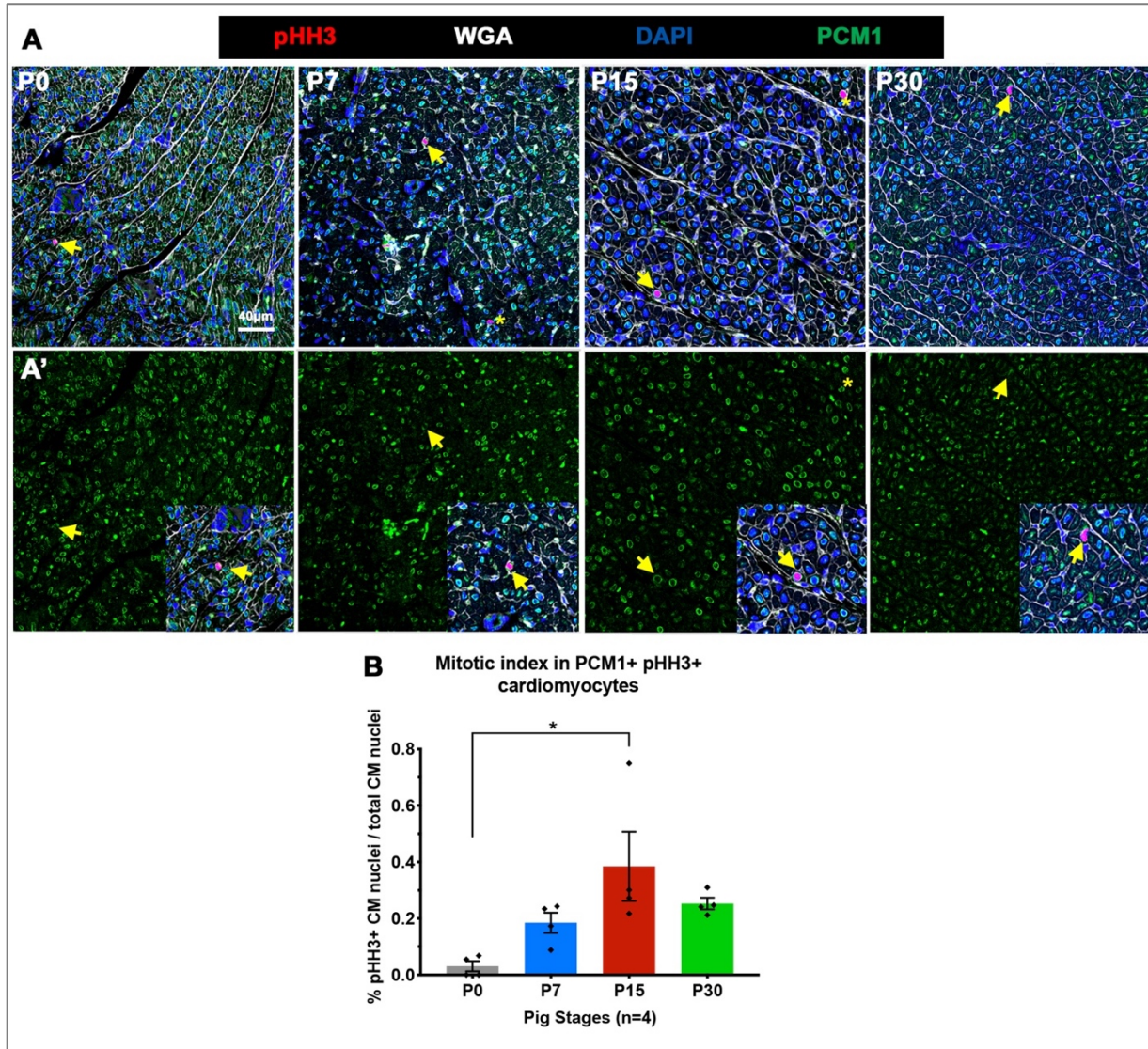
qPCR analysis for cardiac contractile protein isoform switching from fetal (*Tnni1* and *Myh7*) to mature (*Tnni3* and *Myh6*) genes, with fold change calculated relative to P0, in mouse ventricular mRNA. Data are mean \pm SEM, with * $p < 0.05$, ** $p < 0.01$, **** $p < 0.0001$ determined by Dunn's Kruskal-Wallis Multiple Comparisons Tests, in $n = 3-6$ mice per stage. Asterisk(s) with underline indicate significance compared to P0.

Figure S2.



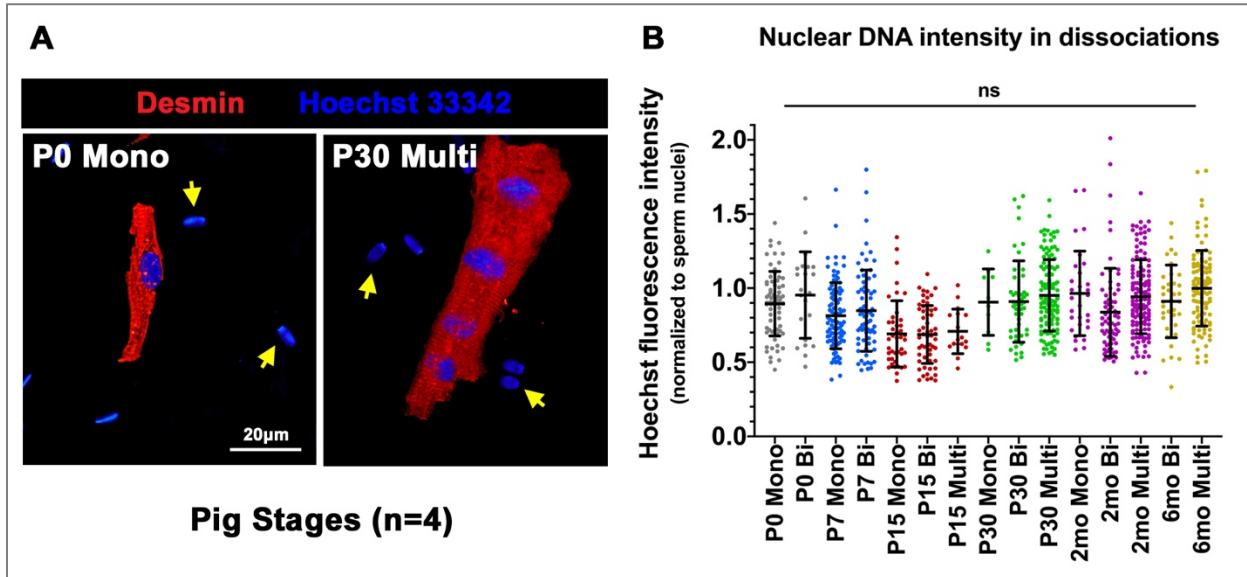
S2. Postnatal pig hearts significantly increase in size beyond P30. (A) Representative images of postnatal pig hearts at birth (P0), one- (P30) and six-months (6mo) post-birth, with relative sizes in centimeters (cm). **(B)** Heart weights were measured in grams (g) at P0-6mo in pigs. **(C)** Total body weights were measured in kilograms (kg) at P0-6mo in pigs. **(D)** Myocardial histology was analyzed by Wheat Germ Agglutinin (WGA), with DAPI staining of nuclei. Red arrows indicate cross-sections of cardiomyocytes as indicators of cell size expansion. **(E)** The number of nuclei per cross-sectional CM area (0.05mm^2) was assessed by DAPI counts in P0-6mo pig left ventricles. **(F)** Representative images of Connexin-43 (Cx43) staining of gap junction proteins, with split channel images (red) for Cx43. Yellow arrows illustrate the differences in gap junctional maturation, from lateral punctate staining at P0, to co-localization with to CM termini at P30-6mo. Punctate expression of Cx43 is evident until 2mo. Data are mean \pm SEM, with * $p < 0.05$, *** $p < 0.001$ determined by Dunn's Kruskal-Wallis Multiple Comparisons Tests, in $n=4$ pigs per stage.

Figure S3.



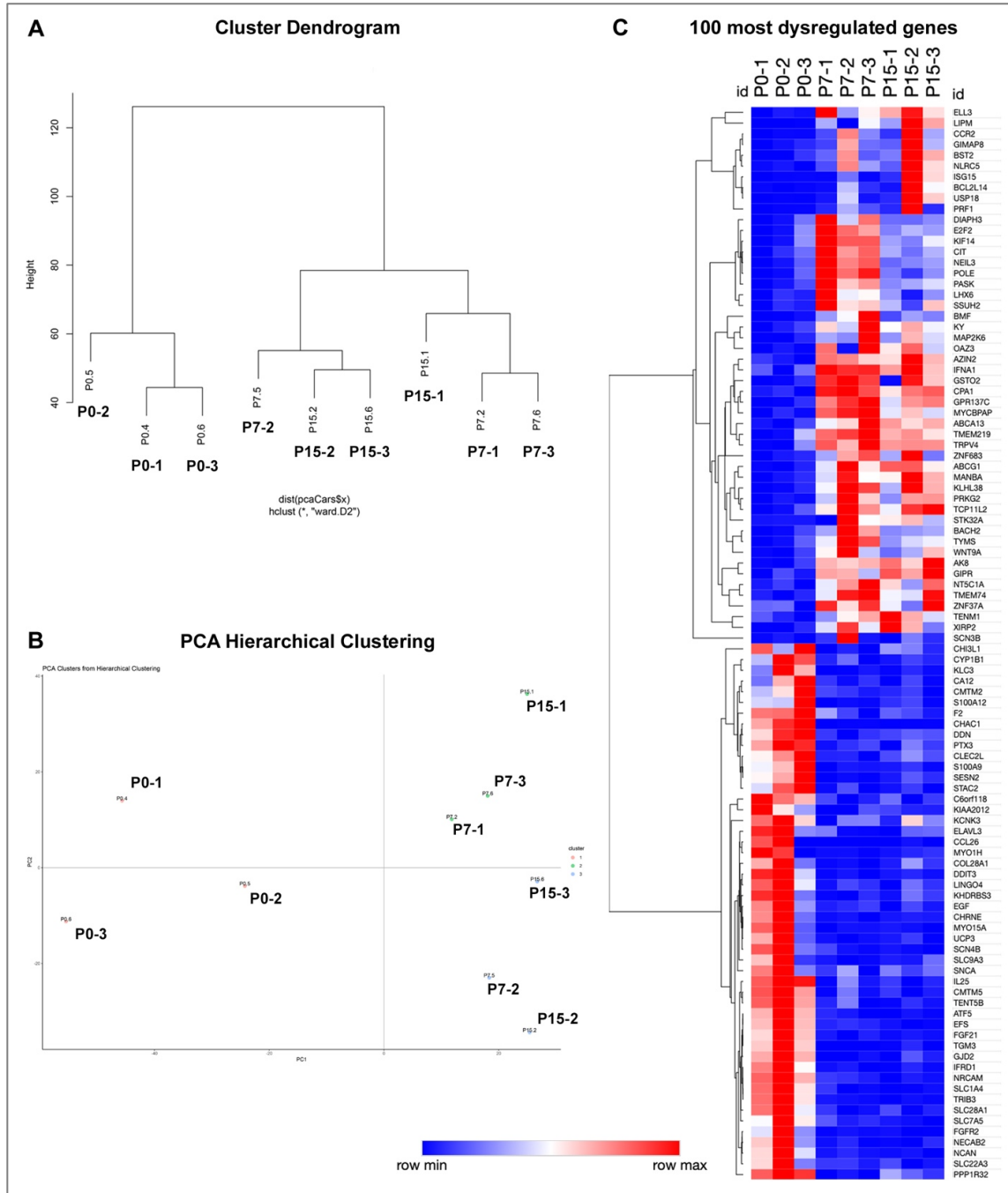
S3. Cardiomyocyte mitotic activity is significantly increased at P15 in pig left ventricles. (A, A') Representative images of Phosphohistone-H3 (pHH3) staining for mitotic activity (A, yellow arrows) in pig heart tissue sections. Cardiomyocyte (CM) nuclei were identified by perinuclear PCM1 (A', green staining), with corresponding pHH3 expression shown in inlaid panel. (B) Ratio of pHH3-positive CM nuclei to total CM nuclei was calculated in cardiac cross-sections. Data are mean \pm SEM, with $*p < 0.05$ determined by Dunn's Kruskal-Wallis Multiple Comparisons Tests, in $n=4$ pigs per stage.

Figure S4.



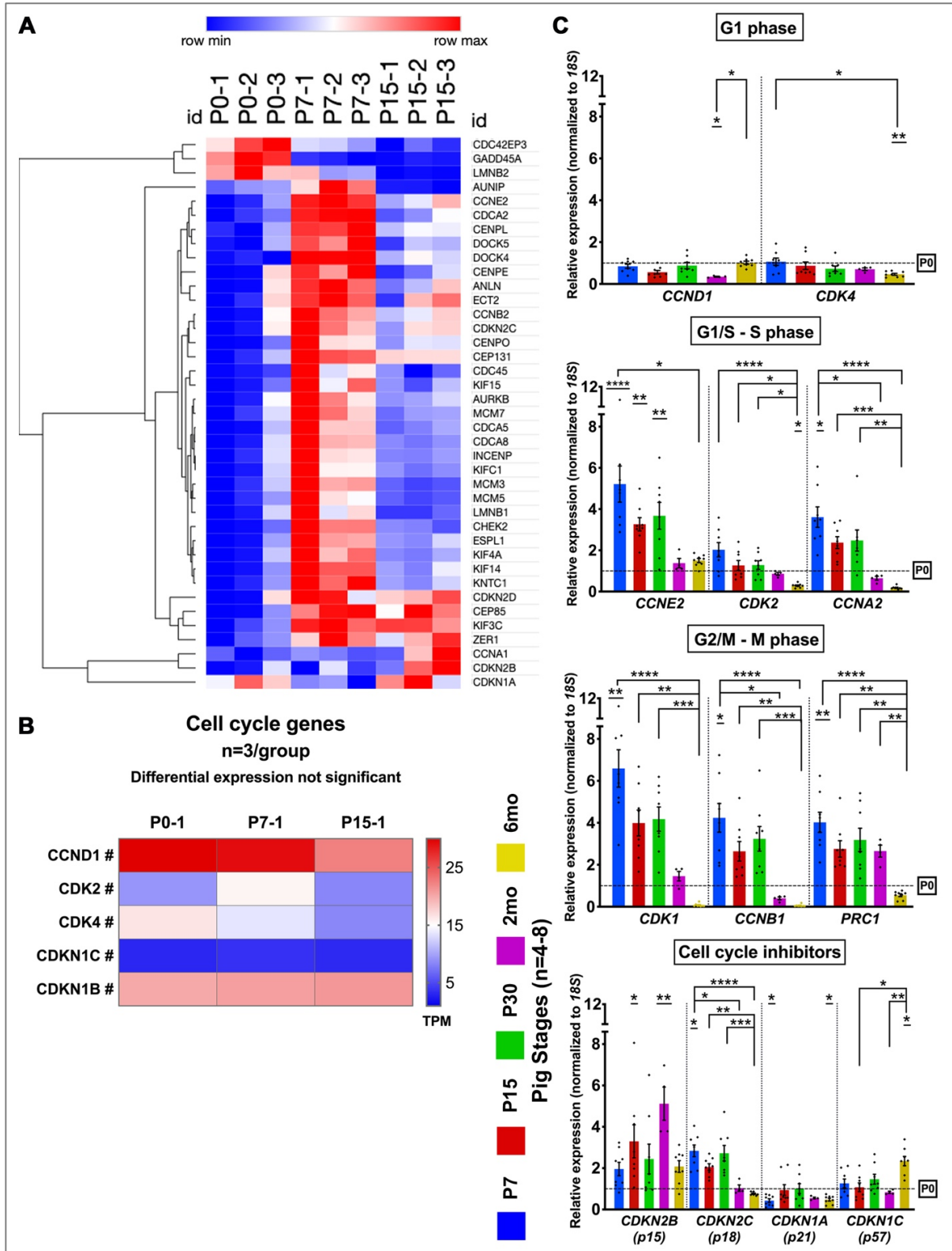
S4. Cardiomyocyte nuclear intensities do not change from birth to 6mo in pigs. (A) Representative images of dissociated CMs stained with Hoechst 33342 for nuclear intensity assessment, with sperm nuclei (yellow arrows) utilized for nuclear intensity normalization per field. **(B)** Hoechst fluorescence intensity per CM nucleus was normalized to sperm nuclear Hoechst intensities per image (>100 CMs counted per stage), to obtain relative intensities as shown (not a measure of nuclear DNA content). Data are mean \pm SEM, with ns=not significant determined compared to 'P0 Mono' group, by Brown-Forsythe and Welch ANOVA tests, in n=4 pigs per stage.

Figure S5.



S5. Transcriptome analysis in pig left ventricles by RNAseq at P0, P7, and P15. (A) Dendrogram of hierarchical clustering showing linkage between samples. **(B)** Principal component analysis showing segregation of biological replicates within each experimental age group. **(C)** Heatmap showing expression of 100 most significantly dysregulated genes (50 upregulated and 50 downregulated), among all experimental comparisons. Significant differentially expressed genes were obtained using a fold change cutoff of 2 and adjusted p-value cutoff of ≤ 0.05 , in $n=3$ pigs per stage.

Figure S6.

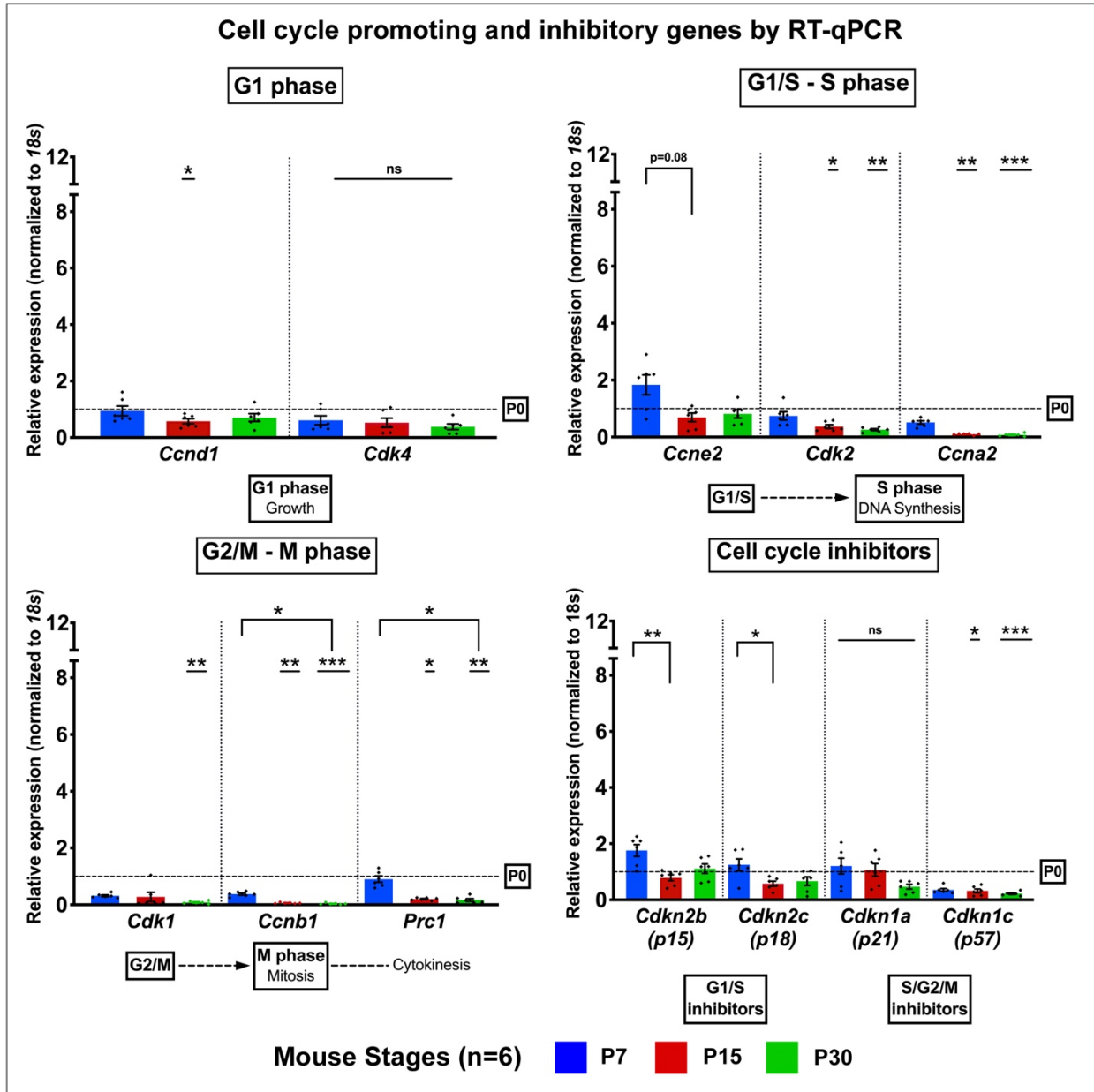


S6. Cell cycle gene expression is not significantly downregulated in the first two postnatal weeks as identified by RNAseq and RT-qPCR in pig left ventricular RNA.

(A) Heatmap showing selected significantly differentially expressed genes involved in cell cycle regulation and mitosis. Significant differentially expressed genes were obtained using a fold change cutoff of 2 and adjusted p-value cutoff of ≤ 0.05 , in n=3 pigs per stage.

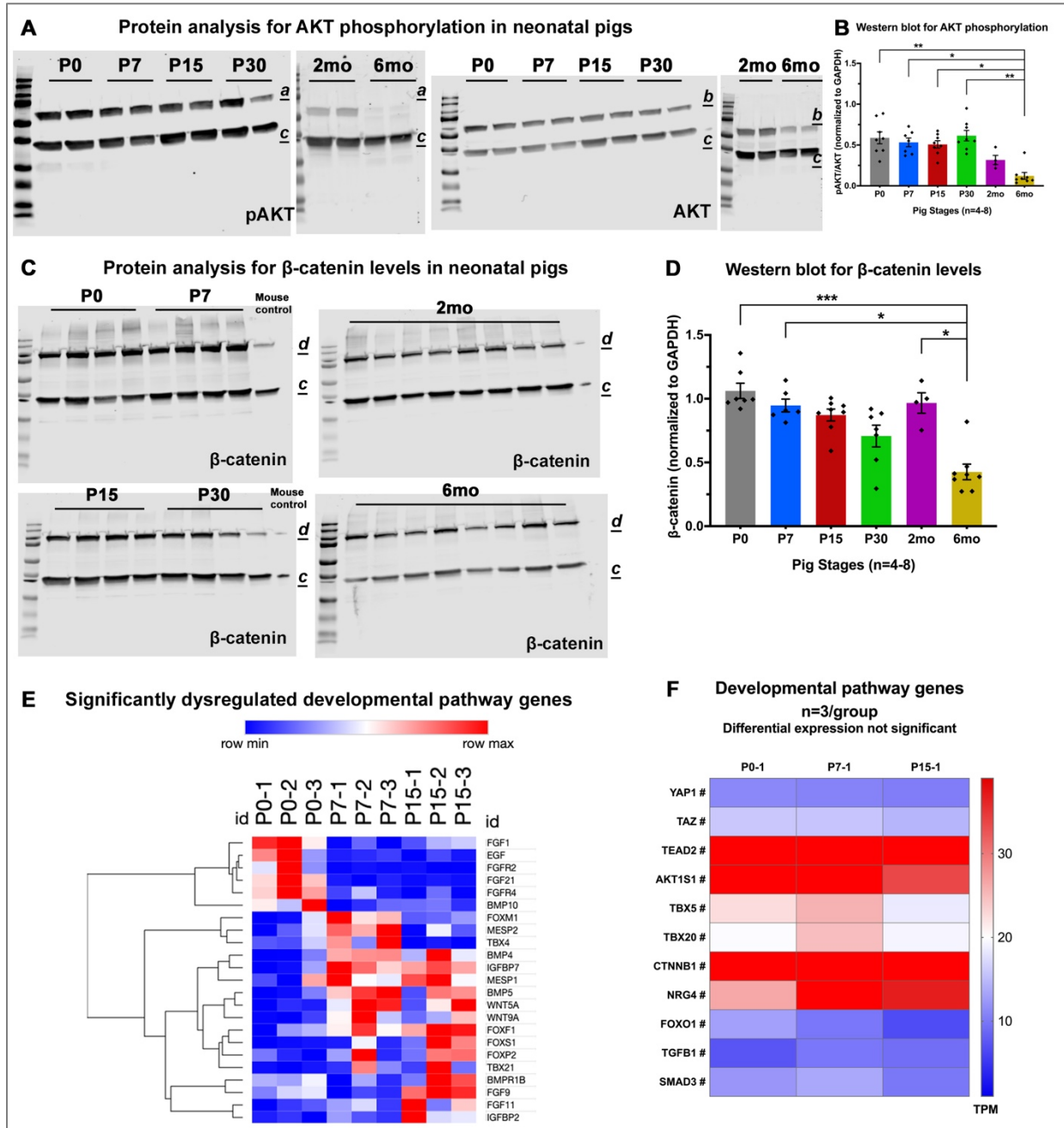
(B) Heatmap showing selected important cell cycle genes, which are not significantly differentially expressed (#) among the three experimental groups. Mean TPM values per stage show continued appreciable expression of key cell cycle regulatory genes in the first two postnatal weeks in pigs. **(C)** RT-qPCR analysis for cell cycle promoting and inhibitory genes, with fold change relative to P0. Data are mean \pm SEM, with *p<0.05, **p<0.01, ***p<0.001, ****p<0.0001 determined by Dunn's Kruskal-Wallis Multiple Comparisons Tests, in n=4-8 pigs per stage. Asterisk(s) with underline indicate significance compared to P0.

Figure S7.



S7. Cell cycle gene expression is significantly downregulated in the first postnatal week by RT-qPCR in mouse left ventricular RNA. RT-qPCR analysis for cell cycle promoting and inhibitory gene expression with fold change calculated relative to P0, in mouse ventricular mRNA. Data are mean \pm SEM, with * $p < 0.05$, ** $p < 0.01$, *** $p < 0.001$ determined by Dunn's Kruskal-Wallis Multiple Comparisons Tests, in $n = 6$ mice per stage. Asterisk(s) with underline indicate significance compared to P0.

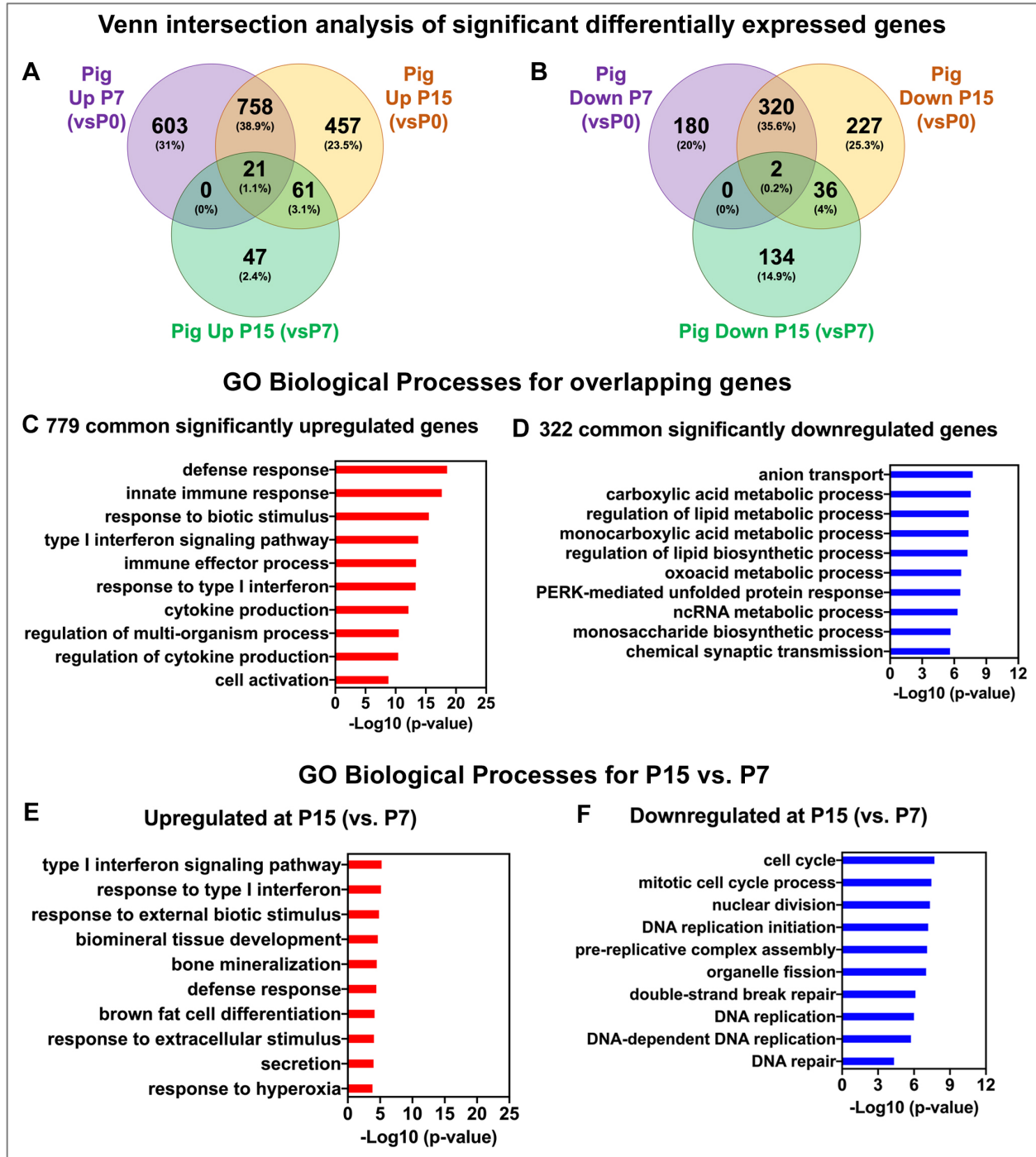
Figure S8.



S8. Cardiac developmental gene expression is active in the first postnatal month in pigs. (A) Representative Western blots for pAKT and AKT levels in pig left ventricular tissue at P0-6mo. a indicates pAKT (60kDa), b indicates AKT (60kDa), with c GAPDH (30-40kDa) utilized for normalization. (B) Ratios of pAKT/ACT assessed from Western quantification normalized to GAPDH. (C) Representative Western blots for β -catenin levels in pig left ventricular tissue, with P30 mouse ventricular protein as control. d indicates β -catenin (100kDa), with c GAPDH (30-40kDa) utilized for normalization. (D) β -catenin levels assessed by Western quantification normalized to GAPDH. Data are mean

± SEM, with *p<0.05, **p<0.01, ***p<0.001 determined by Dunn's Kruskal-Wallis Multiple Comparisons Tests, in n=4-8 pigs per stage. **(E)** Heatmap showing selected significantly differentially expressed cardiac developmental pathway genes, in all three experimental groups by RNAseq. **(F)** Heatmap showing selected important cardiac developmental pathway genes which are not significantly differentially expressed (#) among the three experimental groups. Significant differentially expressed genes were obtained using a fold change cutoff of 2 and adjusted p-value cutoff of ≤0.05, in n=3 pigs per stage.

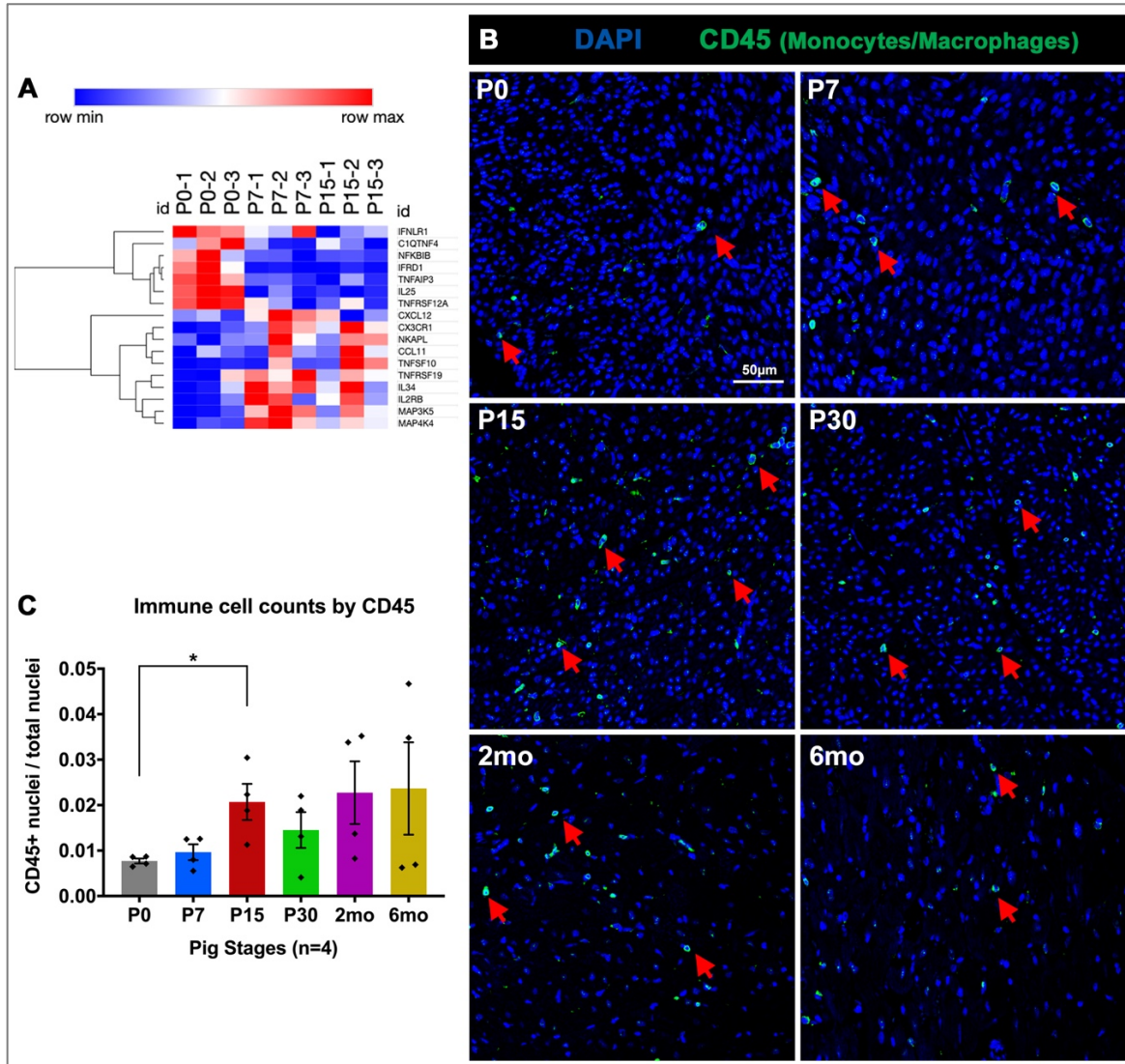
Figure S9.



S9. Gene ontology (GO) analysis of significantly differentially expressed genes by RNAseq. (A) Venn intersection analysis shows total number of significantly differentially upregulated genes and their overlap in P7 vs. P0, P15 vs. P0, and P15 vs. P7 comparison groups. **(B)** Gene Ontology enrichment analysis was performed to get top Biological Process (GO-BP) terms for upregulated overlapping genes. 758 overlapping genes

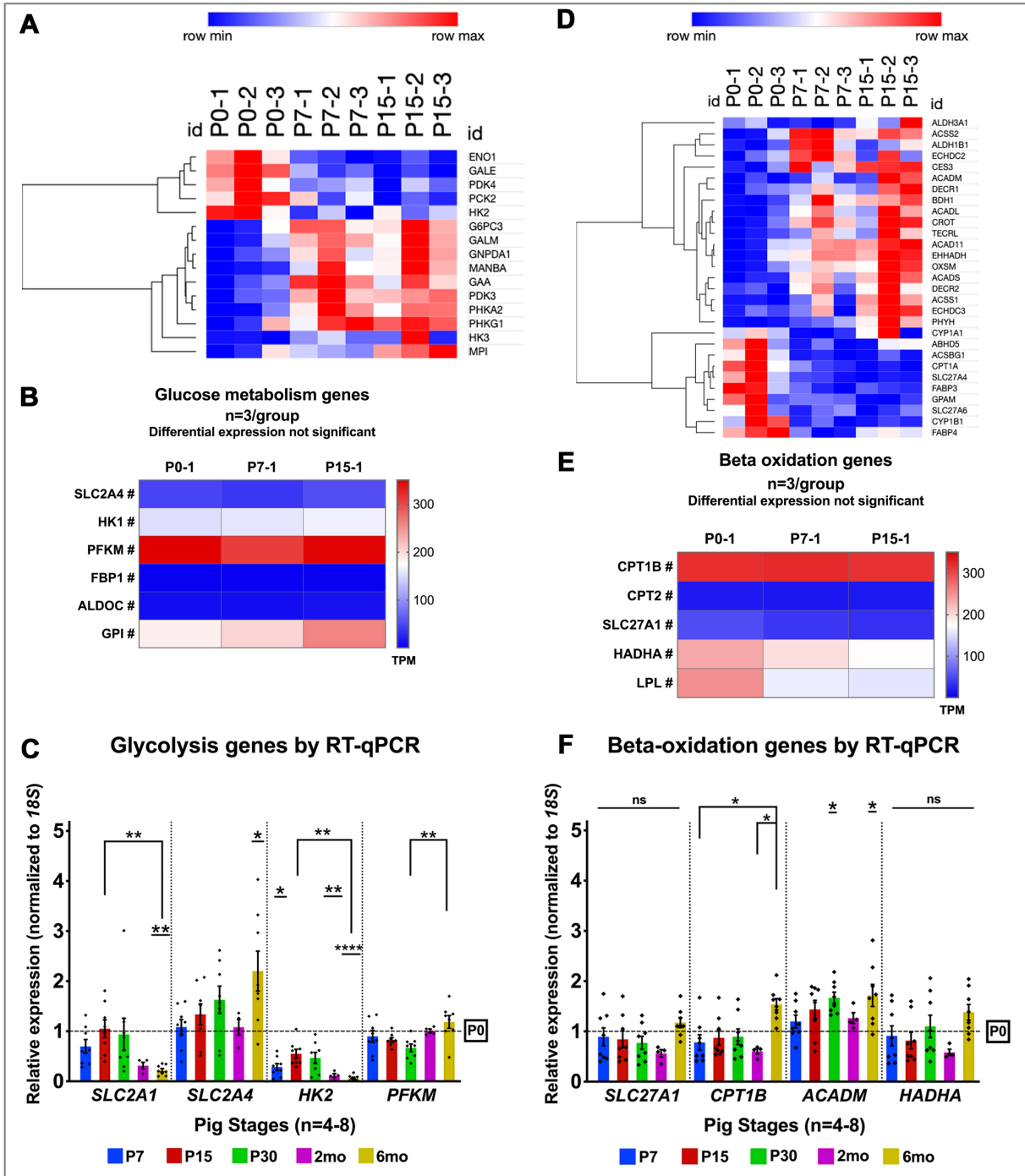
between P7 vs. P0 and P15 vs. P0 comparison groups in addition to 21 overlapping genes between all three comparison groups was chosen to obtain 779 common significantly upregulated genes, during transition from regenerative to non-regenerative state in pigs. **(C)** Venn intersection analysis shows total number of significantly differentially downregulated genes and their overlap in P7 vs. P0, P15 vs. P0, and P15 vs. P7 comparison groups. **(D)** Top GO-BP terms for significantly downregulated overlapping genes. 320 overlapping genes between P7 vs. P0 and P15 vs. P0 comparison groups in addition to 2 overlapping genes between all three comparison groups was chosen to obtain 322 common significantly downregulated genes, during transition from regenerative to non-regenerative state in pigs. **(E, F)** GO term enrichment analysis was performed on all significantly differentially expressed (up- or down-regulated) genes in P15 vs. P7 comparison group. Significant differentially expressed genes were obtained using a fold change cutoff of 2 and adjusted p-value cutoff of ≤ 0.05 . Top GO terms in Biological Processes with $p \leq 0.05$ were selected and plotted for graphical representation.

Figure S10.



S10. Increased innate immune cell gene expression and CD45+ hematopoietic cells by P15 in pigs. (A) Heatmap showing selected significantly differentially expressed genes among all three experimental comparisons by RNAseq, involved in innate immune system response and maturation. Significant differentially expressed genes were obtained using a fold change cutoff of 2 and adjusted p-value cutoff of ≤ 0.05 . (B) Representative images of CD45 (hematopoietic lineage marker, red arrows) staining in pig neonatal heart tissue sections. (C) Ratio of CD45-positive nuclei to total nuclei was calculated. Data are mean \pm SEM, with $*p < 0.05$ determined by Dunn's Kruskal-Wallis Multiple Comparisons Test, in $n=4$ pigs per stage.

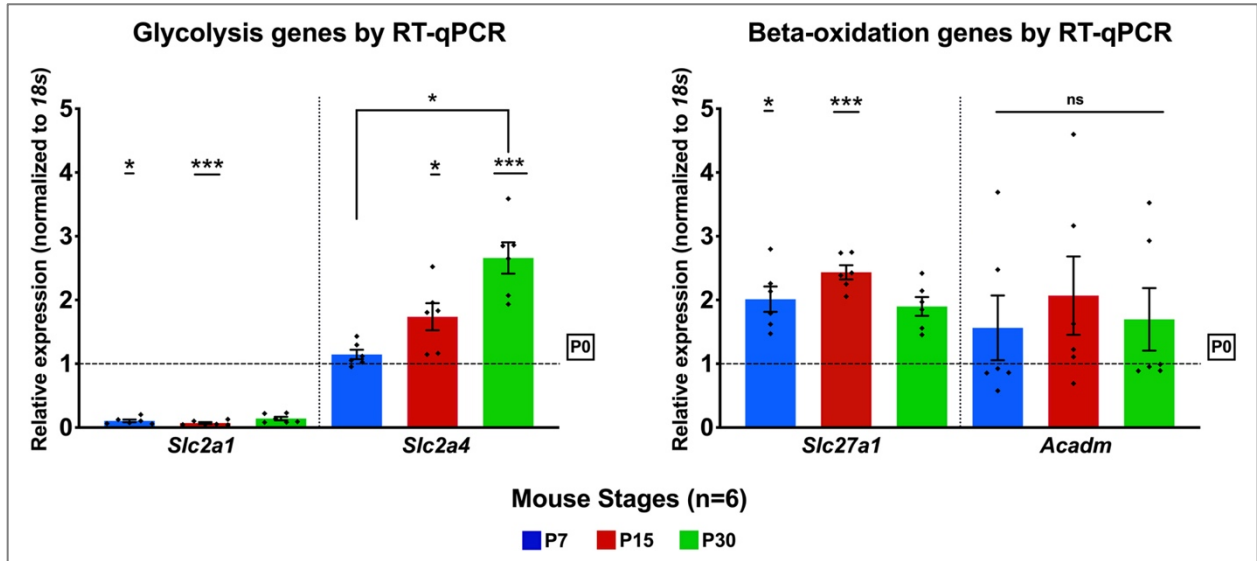
Figure S11.



S11. Metabolic gene expression profiles indicative of transition from glycolysis to beta-oxidation metabolism are not significantly altered at P0-P30 in pigs. (A) Heatmap shows selected significantly differentially expressed glycolysis metabolism genes, among all three experimental comparisons by RNAseq. **(B)** Heatmap shows selected glycolysis genes which are not significantly differentially expressed (#) among the three experimental groups. Mean TPM values per stage show continued appreciable

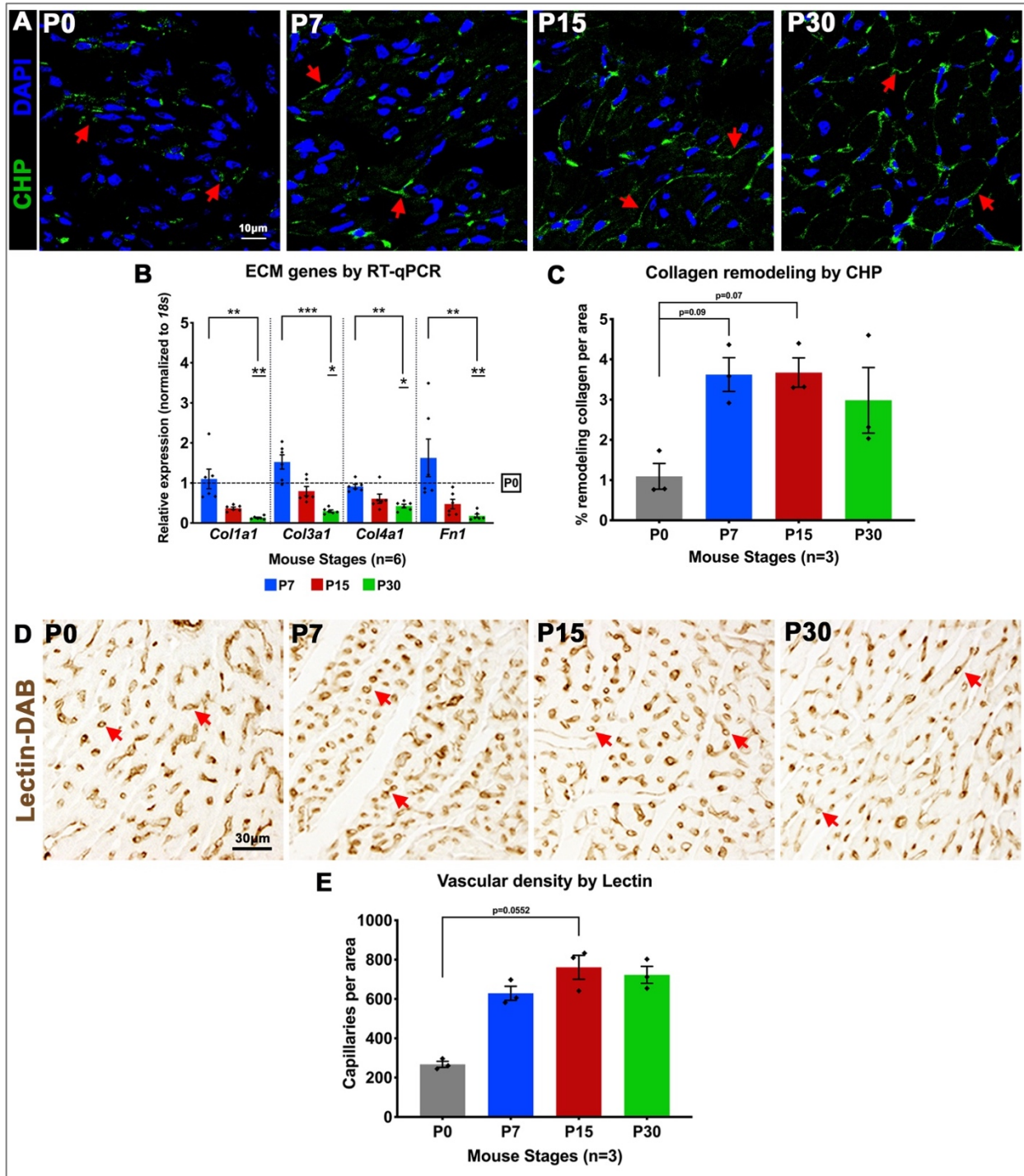
expression of important rate-limiting glycolysis metabolism genes in the first two postnatal weeks in pigs. **(C)** RT-qPCR analysis showing fold change relative to P0 of glycolysis metabolism genes. **(D)** Heatmap shows selected significantly differentially expressed beta-oxidation metabolism genes, among all three experimental comparisons by RNAseq. **(E)** Heatmap showing selected beta-oxidation genes which are not significantly differentially expressed (#). Mean TPM values per stage indicate continued appreciable expression of important rate-limiting beta-oxidation metabolism genes, in the first two postnatal weeks in pigs. **(F)** RT-qPCR analysis showing fold change relative to P0 of beta-oxidation metabolism genes. Significant differentially expressed genes were obtained using a fold change cutoff of 2 and adjusted p-value cutoff of ≤ 0.05 . Data are mean \pm SEM, with * $p < 0.05$, ** $p < 0.01$, **** $p < 0.0001$ determined by Dunn's Kruskal-Wallis Multiple Comparisons Tests, in $n = 4-8$ pigs per stage. Asterisk(s) with underline indicate significance compared to P0.

Figure S12.



S12. Upregulation of mature metabolic gene expression by P7-P15 in mouse ventricles. RT-qPCR analysis in mouse ventricular mRNA for metabolic switching shows downregulation of fetal *Slc2a1* and upregulation of mature *Slc2a4* in glycolytic pathway genes, alongside upregulation in beta-oxidation gene expression, after birth in mice. Fold change was calculated relative to P0. Data are mean \pm SEM, with * $p < 0.05$, *** $p < 0.001$ determined by Dunn's Kruskal-Wallis Multiple Comparisons Tests, in $n=6$ mice per stage. Asterisk(s) with underline indicate significance compared to P0.

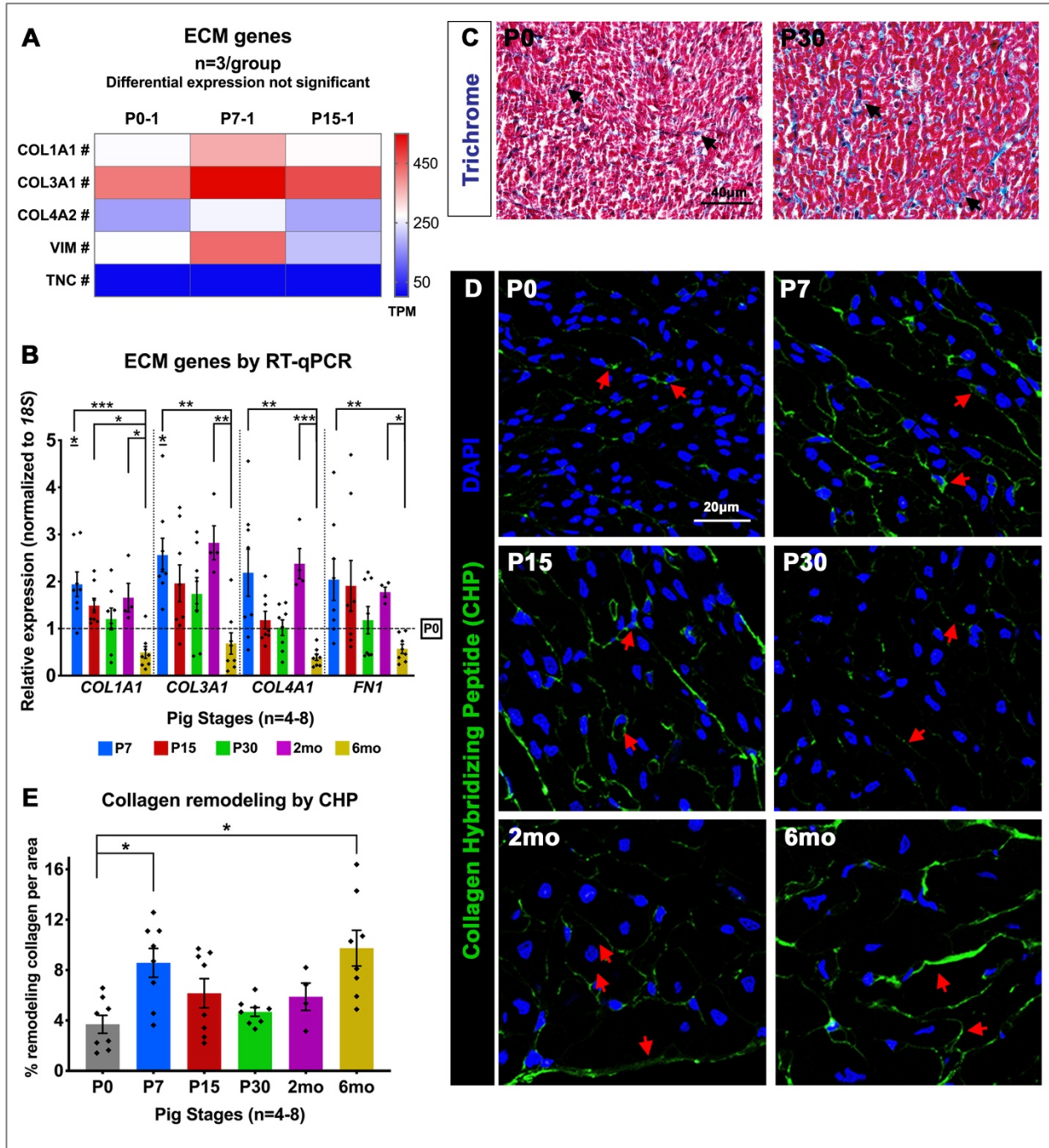
Figure S13.



S13. Postnatal extracellular matrix maturation and vascular remodeling at P7-P15 in mouse left ventricles. (A) Collagen remodeling was assessed by fluorescent Collagen Hybridizing Peptide (CHP) staining (green staining, red arrows). (B) RT-qPCR analysis of collagen isoform gene expression, with fold change relative to P0. (C) Quantification of collagen remodeling by measuring CHP expression (green

fluorescence) per area (0.05mm^2). **(D)** Representative images of circular capillaries (red arrows) identified by Lectin-DAB staining in mouse hearts. **(E)** Vascular density was assessed by manual counts for Lectin-DAB stained capillaries per tissue area (0.3mm^2). Data are mean \pm SEM, with * $p < 0.05$, ** $p < 0.01$, *** $p < 0.001$ determined by Dunn's Kruskal-Wallis Multiple Comparisons Tests, in $n=3$ mice per stage. In B, asterisk(s) with underline indicate significance compared to P0.

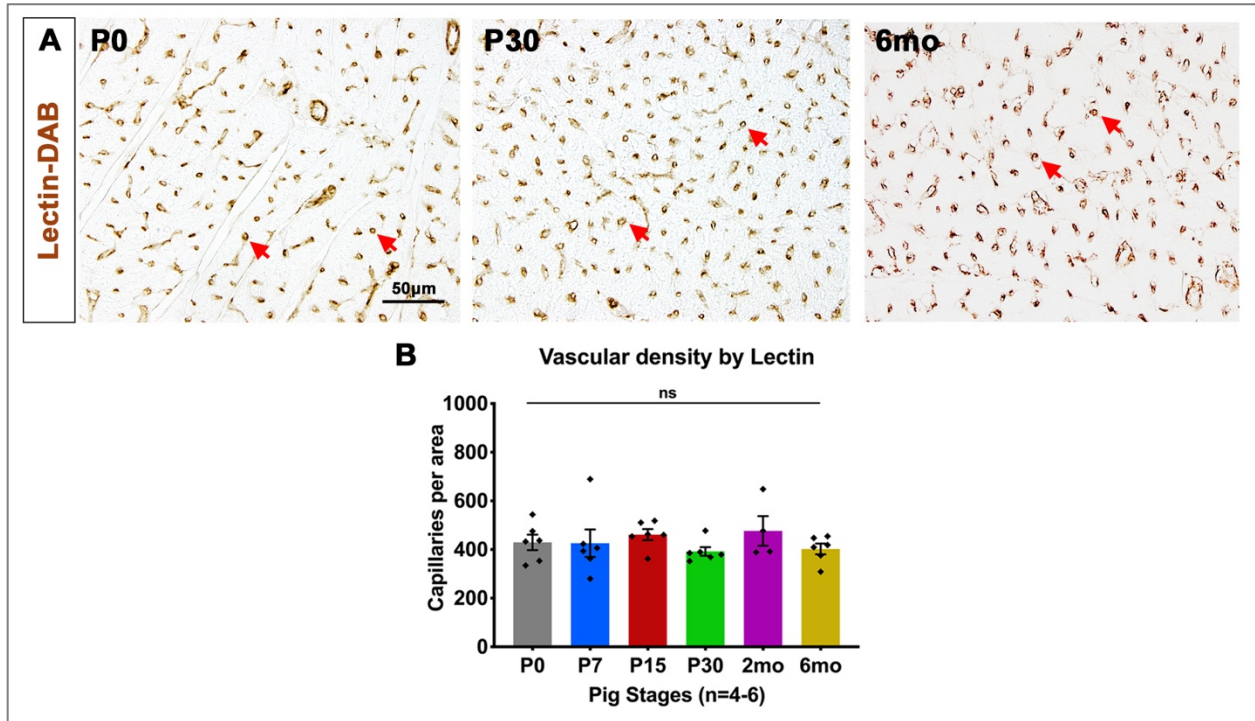
Figure S14.



S14. Increased extracellular matrix remodeling by P7 in pig left ventricles, with ongoing collagen remodeling until 6mo. (A) Heatmap shows selected key extracellular matrix (ECM) genes which are not significantly differentially expressed (#) among the three experimental groups. Mean TPM values per stage show continued appreciable expression of both mature and immature forms of collagen in the first two postnatal weeks in pigs. **(B)** RT-qPCR analysis of collagen and fibronectin isoform genes at P7-6mo with

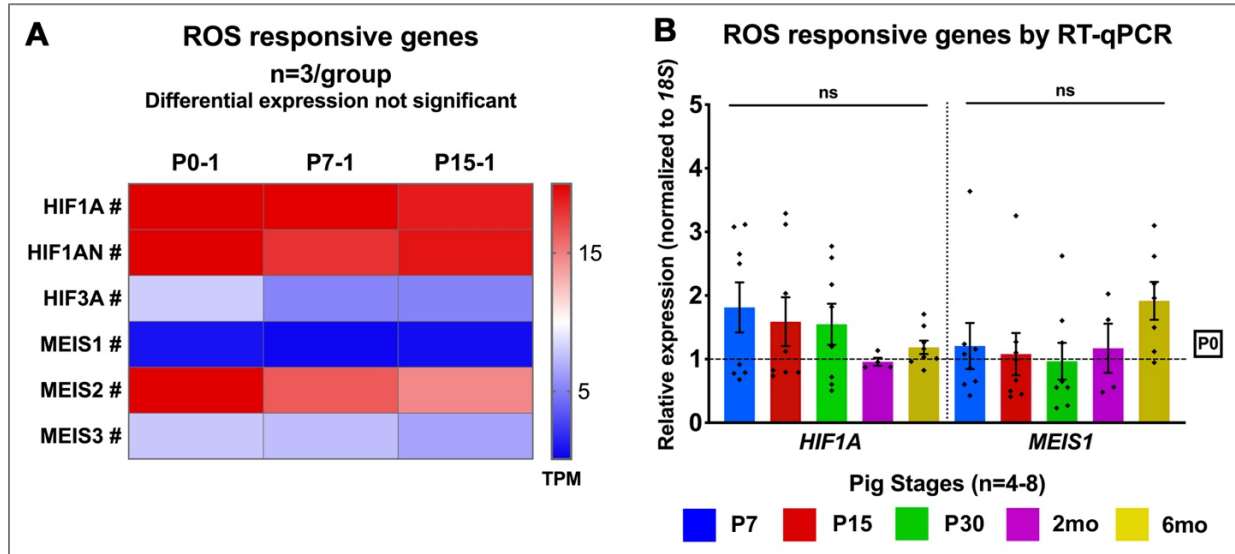
fold change indicated relative to P0 in pig left ventricular mRNA. **(C)** Representative images of Masson's Trichrome staining showing fibrillar collagen (black arrows) at P0 and P30. **(D)** Collagen remodeling was assessed by fluorescent Collagen Hybridizing Peptide (CHP) staining (red arrows). **(E)** Remodeling collagen was quantified as the percent area of CHP expression per total area (0.05mm^2), with significant increase at P7 and 6mo. Data are mean \pm SEM, with * $p < 0.05$, ** $p < 0.01$, *** $p < 0.001$ determined by Dunn's Kruskal-Wallis Multiple Comparisons Tests, in $n=4-8$ pigs per stage. In B, asterisk(s) with underline indicate significance compared to P0.

Figure S15.



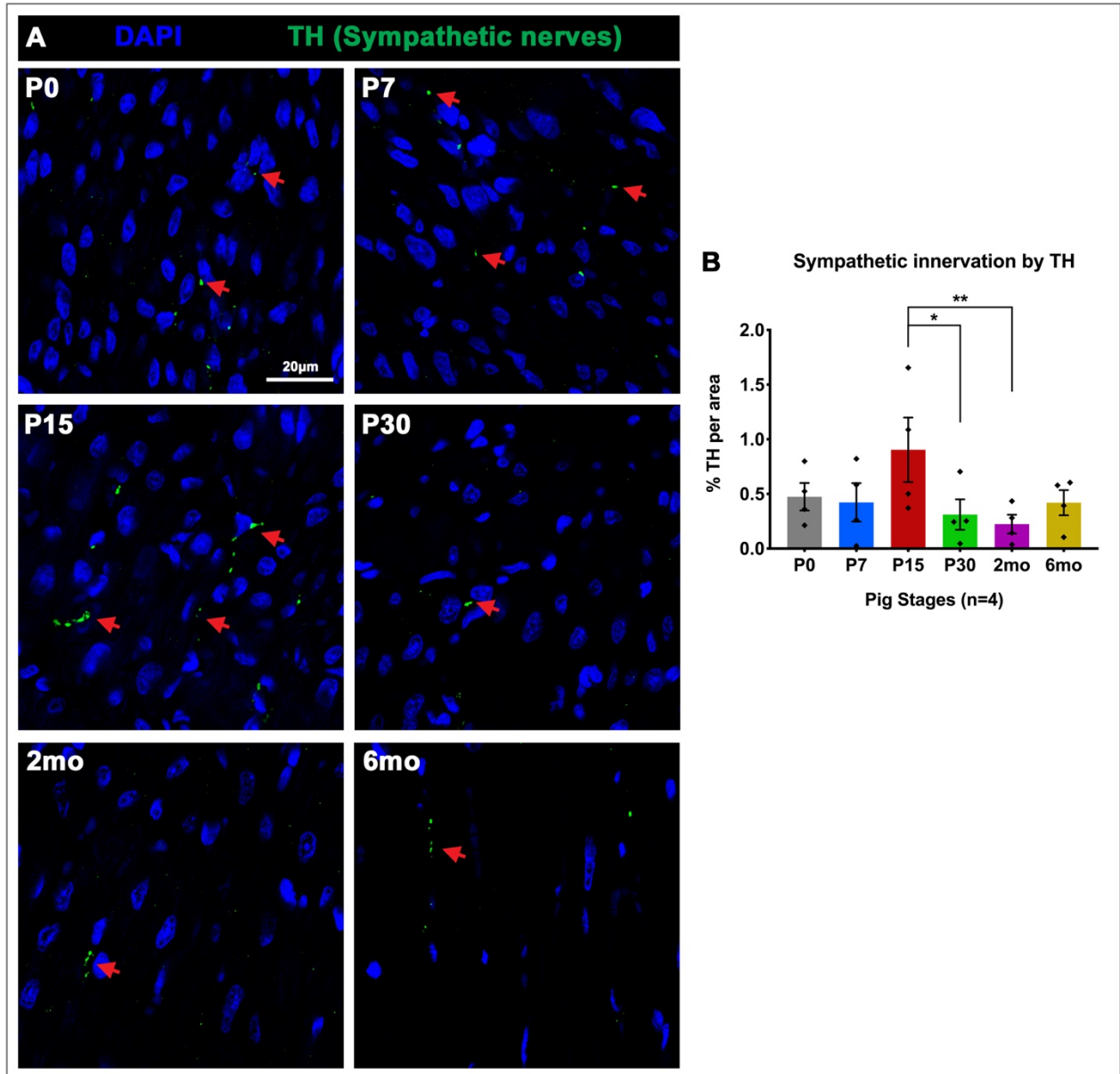
S15. Vascular density does not change after birth in pig hearts. (A) Representative images showing vascular capillaries stained by Lectin-DAB in pig hearts. Red arrows indicate circular capillary structures. (B) Vascular density was assessed by counting Lectin-DAB stained capillaries per area (0.3mm^2). Data are mean \pm SEM, with statistical analysis performed by Dunn's Kruskal-Wallis Multiple Comparisons Tests, in $n=4-6$ pigs per stage.

Figure S16.



S16. Postnatal maintenance of *HIF* and *MEIS* RNA expression in pigs. (A) Heatmap showing selected important ROS responsive genes which are not significantly differentially expressed (#) among the three experimental groups. Mean TPM values per stage show maintenance of expression across the first two postnatal weeks. Significant differentially expressed genes were obtained using a fold change cutoff of 2 and adjusted p-value cutoff of ≤ 0.05 , in n=3 pigs per stage. (B) RT-qPCR analysis of *HIF1A* and *MEIS1* at P7-6mo, with fold change indicated relative to P0 in pig left ventricular mRNA. Data are mean \pm SEM, with statistical analysis by Dunn's Kruskal-Wallis Multiple Comparisons Tests, in n=4-8 pigs per stage (ns=not significant).

Figure S17.



S17. Increased sympathetic neuronal innervation at P15 in pigs. (A) Representative images of postnatal sympathetic neuron signaling in pigs, identified by immunostaining for Tyrosine Hydroxylase (TH, red arrows). **(B)** The presence of sympathetic neurons was quantified as the percent area of TH expression, per total area (0.05mm²). Data are mean \pm SEM, with *p<0.05, **p<0.01, determined by Dunn's Kruskal-Wallis Multiple Comparisons Tests, in n=4 pigs per stage.

Supplementary Tables

Supplementary Table 1. Antibodies and reagents utilized in this study.

Antibodies / Reagents	Catalog No. / Supplier
4',6-diamidino-2-phenylindole (DAPI) [1:10000]	D1306 Thermo Fisher Scientific, Waltham, MA
AKT [1:1000]	9272s Cell Signaling Technology, Danvers, MA
AKT phosphorylated (pAKT) [1:1000]	4058s Cell Signaling Technology, Danvers, MA
Avidin-Biotin (ABC) Kit	PA-6100 Vector Laboratories, Burlingame, CA
Beta (β)-catenin [1:250]	71-2700 Invitrogen, Carlsbad, CA
Bovine Serum Albumin (BSA)	A5611 Millipore Sigma, Burlington, MA
CD45 [1:200]	ab10558 Abcam, Cambridge, UK
cDNA Synthesis Kit SuperScript III First-Strand	11752250 Thermo Fisher Scientific, Waltham, MA
CellLytic MT Cell Lysis Reagent	C3228 Sigma-Aldrich, St. Louis, MO
Citrate Antigen Retrieval Buffer (pH 6.0)	ab93678 Vector Labs, Burlingame, CA
Collagen Hybridizing Peptide (CHP) [20 μ M working]	FLU300 3Helix, Salt Lake City, UT
Collagenase type 2 [4mg/ml working]	LS004174 Worthington Biochemicals, Lakewood, NJ
Collagenase type 4 [1mg/ml working]	LS004186 Worthington Biochemicals, Lakewood, NJ

Connexin-43 (Cx43) [1:300]	ab11370 Abcam, Cambridge, UK
DAB Metal Substrate Kit [1X working]	34065 Thermo Fisher Scientific, Waltham, MA
Desmin [1:200]	ab80503 Abcam, Cambridge, UK
Dispase II [2mg/ml working]	17105041 Thermo Fisher Scientific, Waltham, MA
DNase I enzyme	EN0255 Thermo Fisher Scientific, Waltham, MA
Donkey IgG secondary antibodies [1:500]	Abcam, Cambridge, UK
Donkey Serum	G9663 Sigma-Aldrich, St. Louis, MO
Ethanol	2701, 2801 Decon Labs, PA
Fish Skin Gelatin Blocking	NC0382999 Biotium Inc., Fremont, CA
Formaldehyde	Electron Microscopy Sciences, Hatfield, PA
GAPDH [1:50000]	10R-G109A Fitzgerald Industries, Tompkinsville, KY
Goat IgG secondary antibodies [1:500]	Abcam, Cambridge, UK
Goat Serum	G9023 Sigma-Aldrich, St. Louis, MO
Halt Protease and phosphatase inhibitor cocktail	78440 Thermo Fisher Scientific, Waltham, MA
Hoechst 33342 [1:10000]	H3570 Thermo Fisher Scientific, Waltham, MA
Hydrogen Peroxide	H1009 Millipore Sigma, Burlington, MA

Laemmli sample buffer	1610737 Bio-Rad, Hercules, CA
Lectin (Biotinylated PNA) [1:300]	BA-0074 Vector Laboratories, Burlingame, CA
Masson's Trichrome 2000 Stain Kit	American Master Tech Scientific, McKinney, TX
NucleoSpin RNA Isolation Kit	740955 Macherey-Nagel, Duren, Germany
Odyssey blocking buffer (TBS)	927-50000 Licor, Lincoln, NE
Optimal Cutting Temperature (OCT) Compound	4585 Fisher Scientific, Hampton, NH
Paraformaldehyde (PFA)	Electron Microscopy Sciences, Hatfield, PA
PCM1 [1:200]	HPA023370 Sigma-Aldrich, St. Louis, MO
Phosphohistone H3 (pHH3) [1:100]	06-570 Millipore Sigma, Burlington, MA
Precision Plus Protein™ Dual Color Standards (10-250kDa)	161-0374 Bio-Rad, Hercules, CA
QIAquick Gel Extraction Kit	28704 Qiagen, Hilden, Germany
RiboLock RNase Inhibitor	EO0381 Thermo Fisher Scientific, Waltham, MA
Sarcomeric α -actinin [1:100]	A7811 Millipore Sigma, Burlington, MA
SYBR Green PCR Master Mix	4367660 Thermo Fisher Scientific, Waltham, MA
TissuePrep2 Embedding Media (Paraffin)	8002-74-2 Fisher Scientific, Hampton, NH

Tris Antigen Retrieval Buffer (pH 9.0)	H-3301 Vector Labs, Burlingame, CA
Tris/Glycine/SDS running buffer	1610732 Bio-Rad, Hercules, CA
Tyrosine Hydroxylase (TH) [1:100]	ab112 Abcam, Cambridge, UK
Vectashield Hardset Mounting Medium	H-1400 Vector Labs, Burlingame, CA
Vimentin [1:200]	ab45939 Abcam, Cambridge, UK
Wheat Germ Agglutinin (WGA) 647 [1:250]	W32466 Thermo Fisher Scientific, Waltham, MA
Wheat Germ Agglutinin (WGA) TRITC [1:250]	W849 Thermo Fisher Scientific, Waltham, MA
Xylene	X5-1 Fisher Scientific, Hampton, NH

Supplementary Table 2. Primer sequences used for mRNA analysis by RT-qPCR with SYBR Green.

1A. PIG PRIMERS

Gene Name (Pig)	5' - Forward Primer Sequence - 3' 5' - Reverse Primer Sequence - 3'
<i>18S</i>	AATTCCGATAACGAACGAGACT GGACATCTAAGGGCATCACAG
<i>CCNA2</i>	CCCTGCATTTGGCTGTGAAC ATTCAGGCCAGCTTTGTCCC
<i>CCNB1</i>	CATGCAGGATAATTGTGTGCC CCTCGATTCACCACGACGAT
<i>CCND1</i>	GCGAGGAACAGAAGTGCG TGGAGTTGTCGGTGTAGATGC
<i>CCNE2</i>	TCAAGACGCAGTAGCCGTTT AGCCAAACATCCTGTGAGCA
<i>CDK1</i>	GGAAACCAGGAAGCCTAGCA ACAACGTGTGGGAAAGCTACA
<i>CDK2</i>	AAGTGGGCCAGGCAAGATT GAGCTGCCTTTGCTGAAATCC
<i>CDK4</i>	ATGTGGAGCGTTGGCTGTAT TGCTCCAGACTCCTCCATCT
<i>CDKN1A</i>	ACCATGTGGACCTGTTGCTGT AGAAATCTGTCATGCTGGTCTGCC
<i>CDKN1C</i>	GGTTATGCCAAAGGCACGTC GACTGCAAGCTAGATGGGCT
<i>CDKN2B</i>	ACCGTGCGTCAACTTCTGG CAGAAACCGGGCAACGTCA

<i>CDKN2C</i>	ACCGAACTGGTTTCGCTGTC CTTTGCTGGCGGTATGCTTT
<i>PRC1</i>	GTCAAGCATGGAGCCAATGAG AGAATAGGTGCTGGCAACAGA
<i>COL1A1</i>	CTGGAAGAGCGGAGAATACTG CTGTAGGTGAAGCGGCTGTT
<i>COL3A1</i>	CCTGGACGAGATGGAAACCC GGCTACCTACTGCACCTTGG
<i>COL4A1</i>	TTGGCGGTTCTCCAGGAATC GTCACACCCTGCTGTCCTTT
<i>FN1</i>	ACCCTTGCAGTTCCGAGTTC TCCCTGACGATCCCCTTCT
<i>MYH6</i>	GTGAAGAGATAACCAGAGGAGCG CACCTGATCCTCCTTCACGG
<i>MYH7</i>	AAGGTCAAGGCCTACAAGCG CTTTGTTGCGCCCTCAGGAT
<i>TNNI1</i>	AACTTCACGCCAAGGTGGAG ATGGCCTCGACGTTCTTTCT
<i>TNNI3</i>	ATACGACGTGGAGGCGAAAG CATCATGGCATCGGCAGAGA
<i>HIF1A</i>	CGTGCGACCATGAGGAAATG ACAAATCAGCACCAAGCACG
<i>MEIS1</i>	GGCCGTGTGTTTAGAAGCCT TGCTCCAAGGTGGGACTATG
<i>SLC2A1</i>	ATGCGGGAGAAGAAGGTCAC CACGAACAGCGACACGACA
<i>SLC2A4</i>	GAATGTGTGGCTGTGCCATC TAGCATCCGCAACATACTGGAA

<i>HK2</i>	GGATGGCACAGAGAAAGGCG GCAATGCACTGGACGATGTG
<i>PFKM</i>	ATCCCGTTTGTGGTCATCCC AATATAGGCAGCATCGGCC
<i>SLC27A1</i>	ACCTATCAGGTGACGTGCTG ACTCTGATCCAGAGGCAGGT
<i>CPT1B</i>	AAGTCCTTCACCCTCATCGC TGCCAGCATAGGGTTTGGTT
<i>ACADM</i>	ATAGAACTGGCGAGTACCCTG AGGCACACATCAATGGCTCC
<i>HADHA</i>	ACGAGCTTTGGCTTTCCTGT GCGTACTGGATGTCTTCGT

1B. MOUSE PRIMERS

Gene Name (Mouse)	5' – Forward Primer Sequence – 3' 5' – Reverse Primer Sequence – 3'
<i>18s</i>	TTTCTCGATTCCGTGGGTGG TCAATCTCGGGTGGCTGAAC
<i>Ccna2</i>	CTTGGCTGCACCAACAGTAA ATGACTCAGGCCAGCTCTGT
<i>Ccnb1</i>	AGCAAATATGAGGAGATGTACC CGACTTTAGATGCTCTACGGA
<i>Ccnd1</i>	AGTGCGTGCAGAAGGAGATT CACAACTTCTCGGCAGTCAA
<i>Ccne2</i>	ATGTCAAGACGCAGCCGTTTA GCTGATTCCTCCAGACAGTACA
<i>Cdk1</i>	GTCCGTCGTAACCTGTTGAG TGACTATATTTGGATGTCGAAG

<i>Cdk2</i>	TTTGCTGAAATGGTGACCCG GGCTGAAATCCGCTTGTTGG
<i>Cdk4</i>	CGTGAGGTGGCCTTGTTAAG GTACCAGAGCGTAACCACCA
<i>Cdkn1a</i>	CGAGAACGGTGGAACCTTGAC CCAGGGCTCAGGTAGACCTT
<i>Cdkn1c</i>	TCAGCCAGCCTTCGACCAT TTGAAGTCCCAGCGGTTCTG
<i>Cdkn2b</i>	CCTTTCAGGACGCGGTGTAA CTGACTGCACCCACCCAAAT
<i>Cdkn2c</i>	ACCATCCCAGTCCTTCTGTCA AGAAGCCTCCTGGCAATCTC
<i>Prc1</i>	AAGGAGCTGAGTACCCTGTG CAGAGGATGTCACGGAGTTCT
<i>Col1a1</i>	CTGGCCTCCCTGGAATGAAG GCTTCACCCTTAGCACCAACT
<i>Col3a1</i>	GGACACAGAGGCTTTGATGGA CCACCAGGACTGCCGTTATT
<i>Col4a1</i>	TCATTAGCAGGTGTGCGGTT GCAGAGGCGAGCATCATAGT
<i>Fn1</i>	GGAGCCTTCACACATCACCA AGCGTGTCACTTCTCTGTGG
<i>Myh6</i>	CCTCAAGCTCATGGCTACAC GCTGGGTTTCAGGATGCGATA
<i>Myh7</i>	TTACTTGCTACCCTCAGGTGG CAGTCACCGTCTTGCCATTCT
<i>Tnni1</i>	TTCAGGACTTGTGCCGAGAG TACAGCAAGCCAACCTCTACTG

<i>Tnni3</i>	TCTGCCAACTACCGAGCCTAT CTCTTCTGCCTCTCGTTCCAT
<i>Slc2a1</i>	CTCTGTCTGGCCTCTTTGTTAAT CCAGTTTGGAGAAGCCCATAAG
<i>Slc2a4</i>	GGACCGGATTCCATCCCAC TCCCAACCATTGAGAAATGATGC
<i>Slc27a1</i>	CGCTTTCTGCGTATCGTCTG GATGCACGGGATCGTGTCT
<i>Acadm</i>	ATGCCTGTGATTCTTGCTGGA ACATCTTCTGGCCGTTGATAAC

Supplementary Table 3. Differential gene expression analyses in pig neonatal left ventricles by RNA sequencing.

(Provided as supplementary Excel file)

Supplementary Methods

This is an expanded section for the methods provided in the main article. Information on antibodies and reagents is provided in Supplementary Table 1, while primer sequences used for RT-qPCR are listed in Supplementary Table 2. RNAseq differential gene expression analyses are available as Supplementary Table 3.

A) Animals

All experiments involving animals were performed conforming to the NIH Guide for the Care and Use of Laboratory Animals and all protocols involving animals were approved by the Cincinnati Children's Hospital Institutional Animal Care and Use Committee (IACUC).

A1) Pigs

A total of n=68 White Yorkshire-Landrace farm pigs were utilized in this study, at ages P0 (postnatal day 0), P7, P15, P30, 2mo (2 months post-birth) and 6mo. The distribution of pigs was as follows: n=14 per stage at P0 to P30, n=4 at 2mo, and n=8 at 6mo. P0 to P30 pigs were purchased from Michael Fanning Farms, (Howe, IN), 2mo pigs from Isler Genetics (Prospect, OH), and 6mo pig hearts were obtained from a local abattoir. Litters of pigs were not weaned until 3 to 4 weeks after birth. Pig euthanasia and cardiac tissue harvests were conducted off-site at the farm for P0 to P30 and 6mo pigs, with excised heart tissue pieces prepared and transported to the laboratory at CCHMC (Cincinnati, OH). 2mo pigs were transported to in-house vivarium 2 days before harvest for acclimatization and subsequently euthanized for heart harvests. Male and female pigs were analyzed at all stages. Only left ventricular free wall tissue was utilized for all pigs, with tissue harvested from the same approximate area of each heart (middle region of the left ventricle), to avoid apex-to-base variations in study results. Out of n=14 pigs per stage at P0 to P30, ventricular tissue of n=6 per stage was processed for cardiomyocyte (CM) dissociations (detailed in Section F), while tissue from the other n=8 per stage was used for histological staining and RNA/protein isolation. Ventricular tissue from all pigs at 2mo and 6mo stages was used for histological staining, RNA/protein isolation, and CM dissociations.

A2) Heart and body weights in pigs

Body weights were obtained by weighing whole pigs (in kg) prior to removal of the heart on a farm animal weighing scale. Following harvest, exsanguinated total hearts were weighed (in g). Heart weight-to-body weight ratios were calculated on Microsoft Excel and visualized using GraphPad Prism 8. Fold-increases in heart and body weights after birth were calculated at P7-6mo relative to heart and body weights at birth (P0).

A3) Mice

A total of n=48 wildtype FVB/N mice were bred in-house at the vivarium in CCHMC, Cincinnati, OH (founder animals were originally sourced from Jackson Labs, Bar Harbor, ME), and hearts were harvested at P0, P7, P15, and P30 (n=12 hearts per stage). Hearts were processed for tissue staining (n=3 hearts per stage for paraffin sections, n=3 hearts

per stage for cryosections) and mRNA analysis (n=6 hearts per stage). Male and female mice were represented at all stages.

B) Tissue processing

Fresh left ventricular tissue samples from pigs after harvest were washed in 1X phosphate buffered saline (PBS) and subsequently placed in 4% paraformaldehyde (PFA) for tissue staining studies, in 3.7% formaldehyde for CM dissociations, or flash-frozen in liquid nitrogen for mRNA and protein analysis. Fixed hearts in 4% PFA were subsequently embedded in Optimal Cutting Temperature (OCT) compound or dehydrated and embedded in Paraffin wax for cryo- and paraffin-sectioning respectively, as described previously [1]. Microtome sections of 5-7 μ m were obtained, encompassing the epicardium to endocardium in each tissue section per slide. In mice, whole hearts were washed in 1X PBS prior to fixation in 4% PFA, and whole ventricular tissue was flash-frozen in liquid nitrogen for all stages.

C) Histochemical and immunohistochemical staining in tissue sections

Paraffin sections were dewaxed by Xylene washes followed by rehydration with graded ethanol concentrations, as described previously [1]. Brightfield images were obtained using an Olympus BX51 microscope equipped with a Nikon DS-Ri1 camera (Tokyo, Japan).

C1) Trichrome staining

Masson's Trichrome 2000 stain kit was used according to manufacturer's protocol to visualize total collagen in tissue sections. Pigs from P0 to 6mo at n=4 per stage were utilized for histological staining and analysis.

C2) Lectin-DAB staining

Antigen retrieval with citrate buffer (1X, pH 6.0) was carried out using pressure cooker/microwave. Blocking was performed with 0.3% hydrogen peroxide and 6% goat serum for 30 minutes each, followed by overnight incubation with biotinylated lectin at 4°C. Staining was detected by Avidin-Biotin Complexing (ABC) kit following manufacturer protocols, followed by color development by immersion for 1 minute in freshly-prepared 3,3'-diaminobenzidine (DAB) metal concentrate in stable peroxidase. Capillaries were identified as small circular Lectin-DAB positive structures. Vascular density was estimated by counting individual Lectin-DAB positive small capillaries in 20X images of at least 4 random cardiac regions per tissue section (n=4-8 pigs per stage), in two technical replicates. Area per 20X image was measured. Both measurements were performed using Fiji (ImageJ) analysis software. Average number of Lectin-DAB positive capillaries per area (0.3mm²) per pig was assessed for vascular density. In mice, the same protocol as above was followed and tissue slides were processed alongside pig samples. At least 3 random 20X images per slide were measured in n=3 mice per stage.

D) Immunofluorescence staining in tissue sections

Confocal images were captured using a Nikon Eclipse Ti Fluorescence microscope, with NIS elements software (Tokyo, Japan). Paraffin-embedded tissue sections were deparaffinized as described above (Section C). Cryosections were thawed at room

temperature followed by 1X PBS washes. Unless specified otherwise, 1X citrate buffer antigen retrieval was performed using pressure cooker/microwave for 20 minutes (paraffin sections) or by incubation of slides for 1 hour at room temperature (cryosections). Unless specified otherwise, blocking was performed using 1X Fish skin gelatin blocking buffer for 1-2 hours at room temperature.

D1) Cardiac morphology and ventricular nuclear density assessment

Paraffin sections following deparaffinization and antigen retrieval were stained with Wheat Germ Agglutinin Alexa Fluor 647 conjugate (WGA 647, cell membrane) and DAPI (nuclei), in order to visualize cardiac morphology in pigs (n=4 per stage) and mice (n=3 per stage). Approximate ventricular nuclear density (number of nuclei per area) per stage in pigs was measured in regions of CM cross-sections in the heart only, to avoid false-counts due to multinucleation. Nuclear density was assessed by Object Counts for individual nuclei via DAPI (blue) pixel identification in NIS Elements software, in 60X images of 4 random cross-sectional cardiac regions per tissue section (n=4 per pigs per stage). Average number of nuclei per area (0.05mm²) per pig was graphed using GraphPad Prism 8.

D2) Connexin-43 staining for sarcomeric gap junctional maturation

Gap junctional maturation was identified by anti-Connexin-43 (Cx43, a gap junctional protein) staining in cryosections, with anti-Desmin to visualize CM. Thawed and washed cryosections were permeabilized in 0.1% Triton for 15 minutes, followed by blocking in 3% BSA for 1-2 hours. Primary antibody was incubated overnight at 4°C, followed by Donkey IgG secondary antibodies, WGA 647 (cell membrane) and DAPI (nuclei) co-staining. 60X images were obtained in n=4 pigs per stage and n=3 mice per stage to visually assess localization of Cx43 to CM termini identified by WGA membrane staining.

D3) Phosphohistone-H3 staining for cardiomyocyte mitotic activity

Cryosections following citrate antigen retrieval and blocking were stained with anti-Phosphohistone-H3 Ser10 (pHH3) antibody, in combination with anti-Sarcomeric α -actinin to identify CMs, WGA 647 or WGA TRITC to identify cell membranes, and DAPI staining of nuclei. Additional cryosections were stained with PCM1 to identify CM nuclei with WGA 647, and DAPI. Primary antibodies were incubated overnight at 4°C. Goat IgG secondary antibodies were utilized. In 20X images of 4-6 random cardiac regions per tissue section (n=4-8 pigs per stage), and in two technical replicates, pHH3+ CM nuclei as identified by α -actinin or PCM1 were counted manually in NIS Elements software. The total number of nuclei per image was counted by Object Counts of DAPI staining in NIS Elements. Mitotic indices were calculated by ratios of pHH3+ CM nuclei to total CM nuclei and the results visualized on GraphPad Prism 8.

D4) Cardiomyocyte cross-sectional area and nuclear area assessment

Paraffin sections following deparaffinization and antigen retrieval were stained with WGA 647 (cell membrane) and DAPI (nuclei) to assess CM cross-sectional area (CSA, μm^2). Fiji (ImageJ) analysis software was used to measure CSA by individual cell tracing in 20X images of 4 random cardiac regions per paraffin tissue section (n=4-8 pigs per stage), and in two technical replicates. In the same images, area of individual nuclei was

determined by Object Area (μm^2) measurements with DAPI staining in NIS Elements software.

D5) CD45 hematopoietic lineage staining for immune cell counts

Paraffin sections were baked for 1 hour at 60°C , and deparaffinized. Antigen retrieval was performed with 1X Tris buffer and Blocking steps were performed using 3% BSA. CD45 antibody was co-stained with DAPI to identify hematopoietic immune cell populations. CD45-positive nuclei were counted manually in NIS Elements software, in 20X images of at least 3 random cardiac regions per paraffin tissue section in $n=4$ pigs per stage.

D6) Collagen hybridizing peptide staining

Cryosections were rehydrated by 1X PBS washes. Collagen Hybridizing Peptide (CHP) working solution ($20\mu\text{M}$) was freshly prepared by heating to 80°C then cooling in ice for 10-15 seconds. Tissue samples were incubated in CHP working solution overnight at 4°C . CHP conjugated to 5-FAM was visualized with excitation/emission at 495/520nm. Co-staining with DAPI was performed following CHP incubation to visualize nuclei. 60X images of at least 4 random cardiac regions per tissue section ($n=4-8$ pigs per stage), in two technical replicates, were obtained in pigs. CHP area was measured by fluorescence thresholding in NIS elements. Total area per image was measured in NIS elements. The ratio of CHP-stained area to total measured area (0.05mm^2) per image was calculated to obtain the percentage of remodeling collagen per area. In mice, $n=3$ cryosections per stage were processed alongside the pig samples.

D7) Tyrosine hydroxylase (TH) staining for sympathetic neurons

Paraffin sections were baked for 1 hour at 60°C , and deparaffinized. Antigen retrieval was performed with 1X Tris buffer and Blocking steps were performed using 3% BSA. TH antibody was co-stained with DAPI to visualize sympathetic neuronal innervation. 20X images of at least 3 random cardiac regions per paraffin tissue section ($n=4$ pigs per stage) were acquired. Neuronal area was measured by fluorescence thresholding in NIS elements. Total area per image was measured in NIS elements. The ratio of TH-stained area to total measured area (0.05mm^2) per image was calculated to obtain the percentage of sympathetic innervation per area.

E) mRNA analysis by RT-qPCR

Ventricular RNA from $n=4-8$ pigs per stage and $n=6$ mice per stage was isolated for gene expression analysis by quantitative real-time polymerase chain reaction (RT-qPCR). Flash-frozen tissue samples from pig and mouse ventricles harvested as described above (Section B) were stored at -80°C until needed. RNA was extracted using NucleoSpin RNA kit following manufacturer's protocol. Further purification was carried out by treatment with DNaseI/RNase inhibitor cocktail followed by cDNA synthesis using SuperScript III First-Strand Synthesis kit, per manufacturer's protocols. RT-qPCR was performed using SYBR Green. Gene-specific primer sets for pigs and mice (Supplementary Table 2) were designed using NCBI PrimerBlast and validated by Sanger sequencing. Samples were amplified in duplicates for 35 cycles using StepOnePlus Real-Time PCR machine (Applied Biosystems). Relative gene expression was calculated by the comparative $\Delta\Delta\text{Ct}$

method [2]. 18S rRNA expression was used for normalization. Normalized average expression of P0 was set to 1.0 to calculate fold change after birth in mice and pigs.

F) Cardiomyocyte dissociations

The protocol of Mollova *et al.* [3] for CM cell dissociation from formalin-fixed tissue was modified for isolating CMs from pig ventricular tissue. Pig heart pieces of roughly 2mm length were excised from ventricular tissue fixed in 3.7% formaldehyde overnight at 4°C, or from tissue stored in 10% neutral-buffered formalin at 4°C. Heart pieces were washed in 1X PBS and subsequently digested by rocking at 37°C for 48 hours in freshly-prepared digestion mixture (4mg/ml Collagenase type 2, 1mg/ml Collagenase type 4, and 2mg/ml Dispase II in 1X PBS). After digestion, eluate was filtered through 200-micron nylon mesh (NC0148096, Fisher) and gently centrifuged at 800rpm for 2 minutes to obtain CM pellets. Resuspended pellets were utilized for antibody staining. Staining steps were performed by repeated centrifugations as described above, followed by pellet resuspensions in appropriate solutions. Following antibody staining, final cell suspensions were pelleted, resuspended in a few drops of Vectashield Hardset mounting medium, deposited onto slides using coverslips, and dried overnight at 4°C before imaging. Individual whole CMs were visually identified based on sarcomeric staining.

F1) Nucleation counts in cardiomyocytes

Dissociated CMs were stained with anti-Sarcomeric α -actinin overnight at 4°C, followed by Goat IgG secondary antibody staining and DAPI. Stained CMs were deposited on slides as described above and confocal images at 20X with at least 10 images per slide and in two technical replicates (n=4-5 pigs per stage) were obtained for assessment of nucleation. The number of nuclei per CM was counted manually in NIS Elements software. Percentages of mono-, bi-, and multinucleated CMs out of total number of CMs counted per pig in each stage was calculated and the results plotted using GraphPad Prism 8.

F2) Cardiomyocyte total surface area, length, and width measurements

CM dissociations were stained with anti-Sarcomeric α -actinin and DAPI as described above. Total surface area per CM (μm^2) was measured after manually tracing cell outlines in at least 6 random 20X images per slide (n=3-5 pigs per stage) and in two technical replicates, using Fiji (ImageJ) software. In the same images, CM lengths and widths (μm) were individually measured by manual tracing of longest (end-end) and widest (middle) points respectively, using Fiji (ImageJ) software. Averages of measurements per pig per stage were calculated and plotted using GraphPad Prism 8.

G) Assessment of nuclear DNA content in dissociated cardiomyocytes and tissue sections

The method of Patterson *et al.* [4] was modified for determination of nuclear DNA content in pig CMs. Pig CM dissociations prepared as described above were mixed with formalin-fixed adult male farm pig sperm after PBS washes. Dissociated cells were stained with anti-Desmin to identify CMs and Hoechst 33342 for nuclear DNA quantification. Confocal images at 60X were acquired with at least 4 images per slide, in n=4 pigs per stage. Hoechst intensities of each nucleus per image were measured by Hoechst 33342 (blue

stain) thresholding in NIS Elements software. CM versus sperm nuclei were identified manually in each image by Binary Object counting. CM nuclear intensities were then normalized to sperm nuclear intensities (which are set to 1.0), to obtain relative intensity values. The normalized relative intensity values of individual CM nuclei were plotted using GraphPad Prism 8. For assessment of nuclear DNA content in cryosections, antigen retrieval and blocking were performed as described above, and sections were stained with Desmin, Hoechst 33342, Vimentin (non-CM marker), and WGA 647. Primary antibodies were incubated overnight at 4°C, and Donkey IgG secondary antibodies were utilized. Images were acquired at 60X with at least 4 images per slide (n=4 pigs per stage), and Hoechst intensity of each nucleus per image was measured in NIS Elements as described above. Desmin-positive (CM) cell nuclei versus Vimentin-positive (non-CM) cell nuclei and their corresponding nuclear intensities were identified manually by Binary Object counting. Hoechst intensity of each CM and non-CM nucleus per image was then normalized to the average of non-CM (diploid, 2c) nuclear intensities for that image, to obtain normalized relative intensity values. Normalized relative nuclear intensity values close to 1.0 in this analysis indicate 2c DNA content. The normalized relative intensity values of individual CM and non-CM nuclei were plotted using GraphPad Prism 8. Based on standard deviation of non-CM relative nuclear intensity values from P0-6mo, thresholds were allotted as: below 1.3 (2c) and above 1.3 (>2c), no units. In longitudinal sections, multinucleated CMs were identified to similarly measure individual nuclear intensities within each multinucleated CM. Utilizing the above thresholds, the percent of nuclei with normalized relative Hoechst intensity values at 2c (below 1.3) or >2c (above 1.3) was calculated for each pig per stage, and the results presented using GraphPad Prism 8.

H) RNA-Sequencing

Total RNA isolated from pig left ventricular myocardial tissue as described above (Section E) at P0, P7, and P15 (n=3 per stage) was used. RNA sequencing (RNA-seq) was performed using the NovaSeq 6000 system in collaboration with the CCHMC DNA Core. Total RNA was isolated from pig left-ventricular myocardial tissue at P0, P7, and P15 in triplicate. The libraries were prepared using TruSeq stranded mRNA protocol. All sample/library quality control analysis was carried out on the AATI Fragment Analyzer (Agilent) and quantified using a Qubit fluorimeter (Thermo Fisher Scientific). Adapter dimers in the libraries were removed from the pool using a 1.5% gel and cleaned using the QiaQuick Gel Extraction Kit protocol. The libraries were sequenced to obtain 101 bp with a coverage of 20 million paired sequencing reads.

H1) Gene Expression Data Analysis

The FASTQ files were obtained from the DNA Sequencing and Genotyping Core Facility at CCHMC. Quality control steps were performed to determine overall quality of the reads from the FASTQ files. Upon passing basic quality matrices, the reads were trimmed to remove adapters and low-quality reads using Trimmomatic [5]. The trimmed reads were mapped to the Sscrofa11 (swine) reference genome. Hisat2 was used for reference alignment [6]. In the next step, transcript/gene abundance was determined using Kallisto [7]. A transcriptome index in Kallisto using Ensemble cDNA sequences for the pig was created. This index was then used to quantify transcript abundance in raw counts and

transcripts per million (TPM). The quantified sample matrix was used for determining differential gene expression between different experimental groups and to profile expression of a specific transcript across various conditions. The R package RUVSeq [8] was used to perform differential gene expression analysis between groups, with raw counts obtained from Kallisto used as input. Significant differentially expressed genes were obtained using a fold change cutoff of 2 and adjusted p-value cutoff of ≤ 0.05 . Data files are available in the GEO database (GSE145346).

H2) Gene Ontology and Pathway Analysis

Downstream functional annotation (cellular components, molecular function, and biological process) and pathway analysis of genes of interest and significantly dysregulated genes were determined using ToppFun tool from the ToppGene Suite [9]. An adjusted p-value cutoff of ≤ 0.05 was used to select functional annotations and pathways. Heatmaps were generated using Morpheus online tool (<https://software.broadinstitute.org/morpheus>).

I) Western blotting for AKT and β -catenin signaling in pig ventricular protein

Pig ventricular tissue stored in -80°C was utilized. Protein was extracted from pig myocardial tissue by homogenizing in CellLytic MT cell lysis reagent at a ratio of tissue to reagent at 1:20. Phosphatase inhibitor cocktail and protease inhibitor cocktail were added to the cell lysis reagent, followed by centrifugation and collection of protein supernatant. Protein quantification was performed using pre-set BSA program on Direct Detect software (Merck Millipore). Samples ($1.5\mu\text{g protein}/\mu\text{l}$) were prepared in Laemmli sample buffer and Cell lysis reagent. Following denaturation at 85°C for 15 minutes, $20\mu\text{l}$ was run on a 12% Mini-PROTEAN TGX precast gel (Bio-Rad) in Tris/Glycine/SDS running buffer with Precision Plus Protein molecular weight ladder (10–250kDa). Following protein transfer to an Immobilon-FL transfer membrane (Merck Millipore), non-specific binding was blocked by incubation in TBS blocking buffer for 1 hour. Membranes were incubated with primary antibodies: AKT, pAKT, β -catenin, and GAPDH overnight at 4°C . Membranes were then washed and incubated with fluorophore-conjugated secondary antibodies followed by quantification of AKT, pAKT or β -catenin protein levels, relative to GAPDH, using an Odyssey CLx infrared imaging system (Licor). Normalized expression values were plotted as pAKT/AKT and β -catenin levels for $n=4-8$ pigs per stage.

J) Graphical representation and statistics

Statistical analysis and graph preparation were done using GraphPad Prism 8 software. Numerical data are shown as means \pm SEM, unless individual sample distribution is not provided in the graph in which case means \pm SD is displayed (as noted appropriately in figure legends). Statistical significance was determined by unpaired One-way ANOVA non-parametric Multiple Comparisons tests, such as Kruskal-Wallis test with Dunn's corrections or Brown-Forsythe and Welch test with Games-Howell corrections. $p < 0.05$ (*) was deemed significant, with $p < 0.01$ (**), $p < 0.001$ (***), and $p < 0.0001$ (****) also represented.

Supplementary References

- [1] F.L. Xiang, M. Guo, K.E. Yutzey, Overexpression of Tbx20 in Adult Cardiomyocytes Promotes Proliferation and Improves Cardiac Function After Myocardial Infarction, *Circulation* 133(11) (2016) 1081-92.
- [2] K.J. Livak, T.D. Schmittgen, Analysis of relative gene expression data using real-time quantitative PCR and the 2(-Delta Delta C(T)) Method, *Methods* 25(4) (2001) 402-8.
- [3] M. Mollova, K. Bersell, S. Walsh, J. Savla, L.T. Das, S.Y. Park, L.E. Silberstein, C.G. Dos Remedios, D. Graham, S. Colan, B. Kuhn, Cardiomyocyte proliferation contributes to heart growth in young humans, *Proc Natl Acad Sci U S A* 110(4) (2013) 1446-51.
- [4] M. Patterson, L. Barske, B. Van Handel, C.D. Rau, P. Gan, A. Sharma, S. Parikh, M. Denholtz, Y. Huang, Y. Yamaguchi, H. Shen, H. Allayee, J.G. Crump, T.I. Force, C.L. Lien, T. Makita, A.J. Lusic, S.R. Kumar, H.M. Sucov, Frequency of mononuclear diploid cardiomyocytes underlies natural variation in heart regeneration, *Nat Genet* 49(9) (2017) 1346-1353.
- [5] A.M. Bolger, M. Lohse, B. Usadel, Trimmomatic: a flexible trimmer for Illumina sequence data, *Bioinformatics* 30(15) (2014) 2114-20.
- [6] D. Kim, B. Langmead, S.L. Salzberg, HISAT: a fast spliced aligner with low memory requirements, *Nat Methods* 12(4) (2015) 357-60.
- [7] N.L. Bray, H. Pimentel, P. Melsted, L. Pachter, Erratum: Near-optimal probabilistic RNA-seq quantification, *Nat Biotechnol* 34(8) (2016) 888.
- [8] D. Risso, J. Ngai, T.P. Speed, S. Dudoit, Normalization of RNA-seq data using factor analysis of control genes or samples, *Nat Biotechnol* 32(9) (2014) 896-902.
- [9] J. Chen, E.E. Bardes, B.J. Aronow, A.G. Jegga, ToppGene Suite for gene list enrichment analysis and candidate gene prioritization, *Nucleic Acids Res* 37(Web Server issue) (2009) W305-11.